ELSEVIER

Synthesis and quadratic molecular hyperpolarizabilities of two new chiral boronates: Computational and experimental study

Horacio Reyes [a], José María Rivera [a], Norberto Farfán *,[a], Rosa Santillan [a],*,
Pascal G. Lacroix *,[b], Christine Lepetit [b], Keitaro Nakatani [c]

[a] *Departamento de Química, Centro de Investigación y de Estudios Avanzados del IPN, Apdo. Postal 14-740, 07000 México D.F., Mexico*
[b] *Laboratoire de Chimie de Coordination du CNRS, 205 Route de Narbonne, 31077 Toulouse Cedex 04, France*
[c] *Laboratoire de Photophysique et Photochimie Supramoléculaires et Macromoléculaires (UMR8531 du CNRS), Ecole Normale Supérieure de Cachan, Avenue du Président Wilson, 94235 Cachan, France*

Abstract

A monomeric boronate and an oxobridged chiral dimer were obtained by reaction of the ligand derived from 4-diethylamino-salicylaldehyde with (R)-(−)-phenylglycinol, and phenyl boronic acid or boric acid. The compounds were fully characterized by spectroscopic techniques (^1H, ^{13}C, ^{11}B NMR, elemental analyses, IR and masses spectrometry); and their molecular hyperpolarizabilities were investigated by the electric field induced second harmonic (EFISH) technique and semi-empirical calculations. The experimental quadratic hyperpolarizability which is equal to 9.8×10^{-30} cm^5 esu^{-1} at 1.064 μm for the monomeric derivative rises to 19.5×10^{-30} cm^5 esu^{-1} in the dimeric specie.
© 2005 Elsevier B.V. All rights reserved.

1. Introduction

There is a considerable interest in the synthesis and characterization of organoboron compounds due to their interesting applications, for example in medicinal chemistry, as anticancer agents or in Boron Neutron Capture Therapy [1]. Moreover, they also display a wide range of applications in organic synthesis [2], as materials with fluorescence [3], electro-optical and nonlinear optical properties [4].

The design of nonlinear optical (NLO) materials efficient in second harmonic generation (SHG) is usually achieved in two steps which imply first the synthesis of compounds having large β values, according to the following expression of the molecular polarization (μ) induced by a laser electric field (E) [5]:

$$\mu(E) = \mu_0 + \alpha E + \beta E^2 + \cdots \qquad (1)$$

In this expression, μ_0 is the permanent dipole moment, α is the linear polarizability, and β the quadratic hyperpolarizability, the origin of the NLO response. The largest β values are obtained when the molecules contain π-electron systems with charge asymmetry arising from the use of donor and acceptor substituents [6]. Ultimately, the NLO response of a macroscopic material is related not only to β, but also to the relative orientation of molecules in the solid state (second step). A non-centrosymmetric environment is required to avoid the cancellation of the quadratic property.

In a previous study we reported on the quadratic NLO properties of a series of 18 "push-pull" boronates

* Corresponding author. Tel.: +52 55 5061 3725; fax: +52 55 5061 3389.
E-mail addresses: jfarfan@cinvestav.mx (N. Farfán), rsantill@cinvestav.mx (R. Santillan), pascal@lcc-toulouse.fr (P.G. Lacroix).
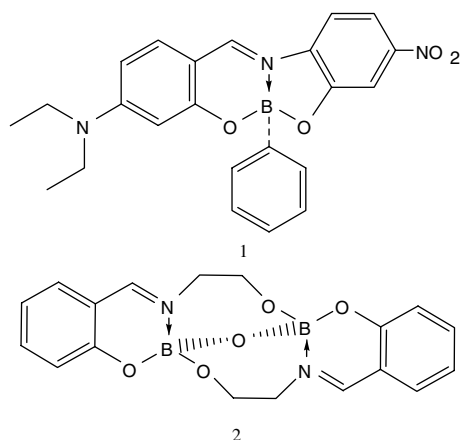
Fig. 1. "Push-pull" boronate **1** and diboronate **2**.

[4b] obtained by self-assembly of salicylideneiminophenols with various phenylboronic acids; in particular, the "push-pull" boronate **1** (Fig. 1) showed a sizeable NLO response in solution. In contrast, most of these boronate derivatives are silent in solid state second harmonic generation (SHG), due to the fact that they crystallize in centrosymmetric space groups. More recently, we reported the synthesis of several dimeric boron complexes with potential application in host–guest chemistry [7] whereby the crystal structure [7c] of oxobridged derivative **2** (Fig. 1) revealed that the compound is strongly bent, with an angle close to 82° between the two phenyl planes (Fig. 2).

The present contribution focuses on the synthesis, structural studies and nonlinear optical properties of the oxobridged boronate **5** (Scheme 1). The new derivative possesses the structural framework of **2**, however, in order to increase the NLO response, two diethylamino electron donor groups were introduced in the salicylidene moiety, *para* to the carbon nitrogen double bond. Additionally, two asymmetric carbons were introduced in the molecular structure by the use of enantiomerically pure *R*-(−)-phenylglycinol as the starting material, to ensure a non-cen-

trosymmetric structure for **5**, and hence solid state SHG efficiency. The properties of diboronate **5** were compared with those of the related mono-boronate **4a**. Moreover, due to the fact that all attempts to crystallize **5** and **4a** were unsuccessful, the calculated molecular structures were compared with the experimentally determined X-ray structures of compounds **2** and **4b**, whereby the latter was prepared in this study. The experimental NLO properties of **5** and **4a** are reported and analyzed on the basis of semi-empirical calculations performed on their calculated molecular structures.
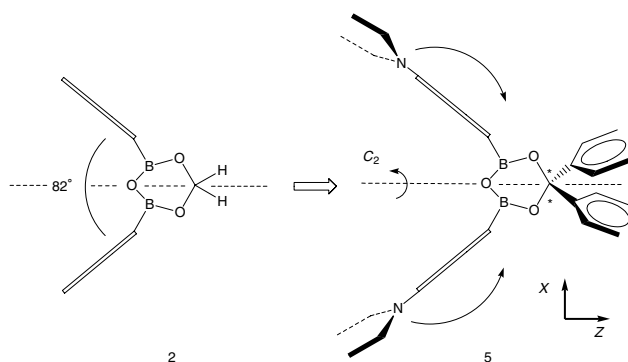
2. Experimental

All starting materials were purchased from Aldrich Chemical Co. Solvents were used without further purification. Melting points were obtained on a Gallenkamp MFB-595 apparatus and are uncorrected. Infrared spectra were measured on a Perkin–Elmer 16F-PC FT-IR spectrometer. ^{1}H, ^{11}B and ^{13}C NMR spectra were recorded on a Bruker Avance DPX 300 spectrometer. Chemical shifts (ppm) are relative to $(CH_3)_4Si$ for ^{1}H and ^{13}C and to $BF_3 \cdot OEt_2$ for ^{11}B. UV spectra were obtained with a Perkin–Elmer Lambda 12 UV/Vis spectrophotometer. Mass spectra were recorded on a HP 5989A spectrometer. Elemental analyses were carried out on a Thermo Finnigan Flash 1112 elemental analyzer.

X-ray crystal structure determination for compound **4b** was obtained on an Enraf Nonius-Fr590 Kappa-CCD ($\lambda_{Mo\,K\alpha}$ = 0.71073 Å, graphite monochromator, T = 293 K, CCD rotating images scan mode). When necessary, absorption correction was performed within the SHELX-A [8] program or by the semi-empirical correction through MULTISCAN procedure (PLATON) [9]. All reflection data set were corrected for Lorentz and polarization effects. The first structure solution was obtained using the SHELX-S-97 program and then SHELX-L-97ver. 34 program [8] was applied for refinement and output data. All software manipulations were done under the WIN-GX [10] environment program set. Molecular perspectives were drawn under ORTEP 3 [11] drawing application. All heavier atoms were found by Fourier map difference and refined anisotropically. Some hydrogen atoms were found by Fourier map difference and refined isotropically, the remaining hydrogen atoms were geometrically modeled and calculated for the refinement. Crystal data for **4b** are summarized in Table 1.

2.1. Synthesis

2.1.1. 5-Diethylamino-2-[(2-hydroxy-(1R)-phenylethylimino)-methyl]-phenol (3a)

Compound **3a** was synthesized from 1.93 g (10.00 mmol) of 4-diethylaminosalicylaldehyde and 1.37 g

Fig. 2. Mono- and di-boronated derivatives under investigation. The oxo-bridged derivatives **2** and **5** are shown in a direction perpendicular to the twofold molecular axis.
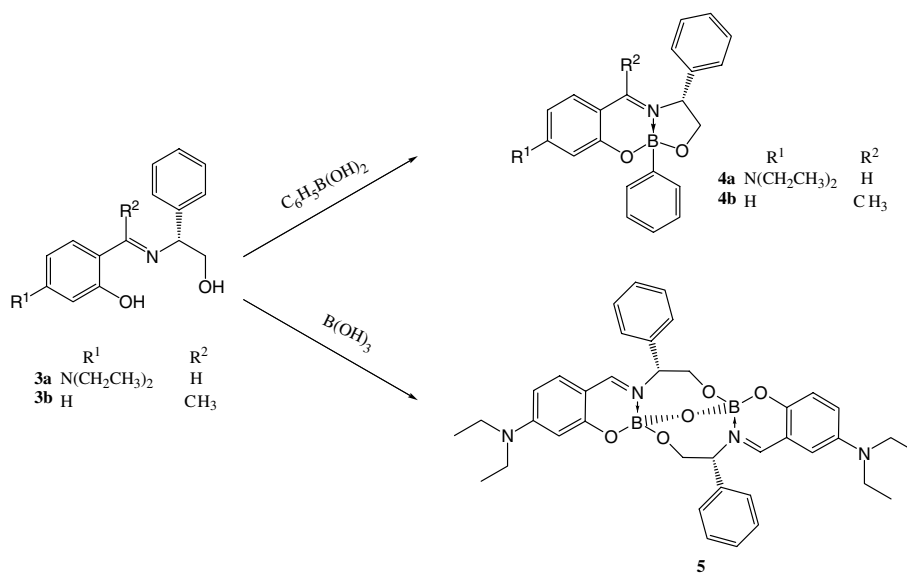
Scheme 1. Synthesis of boronates **4a**, **4b** and **5**.

Table 1
Crystallographic data for compound **4b**

Chemical formula	$C_{22}H_{20}BNO_2$
Formula weight	341.20
Crystal system	Monoclinic
Space group	$P2_1$
Crystal size (mm)	$0.1 \times 0.1 \times 0.1$
a (Å)	8.6473 (2)
b (Å)	10.9323 (3)
c (Å)	10.6276 (3)
β (°)	112.5290 (10)
Formula units per cell	2
δ_{calc} (g cm^{-3})	1.221
$F(000)$	60
Temperature of measurement (K)	293
θ Limits (°)	4.15–27.49
No. of reflections collected	3848
No. of independent reflections	3840
No. of observed reflections, $(F_o)^2 > 4\sigma(F_o)^2$	3108
$R = \sum |F_o| - |F_c|/\sum |F_o|$	0.0393
$R_w = [\sum w(|F_o| - |F_c|)^2 / \sum wF_o^2]^{1/2}$, $w = 1/\sigma^2$	0.0883
Goodness-of-fit σ	1.048
No. of parameters	316
Maximum Δ/σ	0.001
$\Delta\rho_{min}$ (e Å^{-3})	−0.109
$\Delta\rho_{max}$ (e Å^{-3})	0.102

(10.00 mmol) of (*R*)-(−)-phenylglycinol. The reaction mixture was refluxed in toluene for 8 h, using a Dean-Stark trap. The product was obtained as a yellow solid (3.12 g, 9.9 mmol) in 99% yield, m.p. 145–147 °C. IR υ_{max} (KBr): 2958, 1890, 1632 (C=N), 1565, 1307, 1156, 1098, 1020, 765, 530, cm^{-1}. ^{1}H NMR (300 MHz, CDCl$_3$) [δ, ppm]: 1.20 (t, 6H, J = 7.10 Hz, CH$_3$), 3.39 (q, 4H, J = 7.10 Hz, CH$_2$), 3.93 (d, 1H, J = 8.98 Hz, H-8), 4.44 (t, 2H, J = 8.98 Hz, H-9), 6.08 (d, 1H, J = 8.08 Hz, H-3), 6.15 (dd, 1H, J = 2.01 Hz, J = 8.08 Hz, H-5), 7.07 (d, 1H, J = 8.08 Hz, H-6), 7.26–7.40

(m, 5H, H-11, H-12, H-13, H-14, H-15), 8.12 (s, 1H, H-7). ^{13}C NMR (75.46 MHz, CDCl$_3$) [δ, ppm]: 13.1 (CH$_3$), 45.2 (CH$_2$), 68.1 (C-8), 74.0 (C-9), 98.5 (C-5), 104.8 (C-6), 108.6 (C-1), 127.0 (C-11, C-15), 127.8 (C-12, C-14), 129.1 (C-13), 135.8 (C-4), 140.16 (C-10), 152.3 (C-2), 164.8 (C-7). MS (*m/z*, %): 658 (5), 509 (4.4), 453 (5), 379 (3), 321 (100), 308 (57), 277 (13.1), 204 (12.6), 91 (98). Anal. calc. for: C$_{38}$H$_{46}$N$_4$O$_5$B: C, 69.11; H, 7.02; N, 8.48. Found: C, 69.00; H, 7.05; N, 8.22%.

2.1.2. 2-[1-(2-Hydroxy-(1R)-phenyl-ethylimino)-ethyl]-phenol (3b)

A solution of 2-hydroxyacetophenone (1.00 g, 7.34 mmol) and (*R*)-(−)-phenylglycinol (1.00 g 7.34 mmol) in ethanol (150 mL) was refluxed during 1 h using a Dean-Stark trap. The product was obtained as a yellow solid (1.85 g, 7.24 mmol) in 98% yield, m.p. 95–97 °C. IR υ_{max} (KBr): 3059 (OH), 2839, 1611 (C=N), 1449, 1340, 1285, 1149, 1068, 845, 753, 701, 636, 565, 524, 444 cm^{-1}. ^{1}H NMR (300 MHz, CDCl$_3$) [δ, ppm]: 2.36 (s, 3H, CH$_3$), 3.94–3.97 (m, 1H, H-8), 3.97–4.12 (m, 1H, H-9a), 4.96–5.02 (m, 1H, H-9b), 6.77–6.82 (t, 1H, J = 8.0 Hz, H-5), 6.96–6.99 (d, 1H, J = 8.0 Hz, H-3), 7.26–7.38 (m, 6H, H-4, H-6, H-11, H-12, H-13, H-14, H-15), 7.50–7.53 (dd, 1H, J = 8.0 Hz, 3.0 Hz, H-6). ^{13}C NMR (75.46 MHz, CDCl$_3$) [δ, ppm] 15.64 (CH$_3$), 65.69 (C-8), 68.57 (C-9), 117.56 (C-5), 118.98 (C-3), 119.54 (C-1), 127.52 (C-12, 14), 128.10 (C-6), 128.85 (C-13), 129.17 (C-11, 15), 133.18 (C-4), 139.26 (C-10), 164.21 (C-2), 173.96 (C-7). MS (*m/z*, %): 255 (M$^+$, 28), 240 (3), 224 (100), 209(7), 183 (9), 165 (11), 146 (9), 136 (23), 120 (42), 103 (15), 91 (31), 77 (17). Anal. calc. for C$_{22}$H$_{20}$BNO$_2$: C, 75.27; H, 6.71; N, 5.49. Found: C, 75.11; H, 6.52; N, 5.33%.

2.1.3. (5R)-2-(Phenyl)-4-diethylaminobenzo[j]-5-phenyl-6-aza-1,3-dioxa-2-boracyclononene-6-ene (4a)

Compound **4a** was synthesized from 0.50 g (1.60 mmol) of **3a** and 0.19 g (1.60 mmol) of phenylboronic acid. The reaction was carried out by refluxing 18 h in toluene, using a Dean-Stark trap. The product was obtained as a yellow solid (0.54 g, 1.36 mmol) in 85% yield, m.p. 197–199 °C. IR v_{max} (KBr): 2937, 2916, 1636 (C=N), 1560, 1463, 1462, 1208, 1157, 1025, 760 cm^{-1}. ^{1}H NMR (300 MHz, CDCl$_3$) [δ, ppm]: 1.10 (t, 6H, $J = 8.0$ Hz, CH$_3$), 3.29 (m, 4H, $J = 8.0$ Hz, CH$_2$), 4.02 (dd, 1H, $J = 11.3$, 9.8 Hz, H-8), 4.40 (dd, 1H, $J = 11.3$, 3.4 Hz, H-9a), 5.06 (dd, 1H, $J = 9.8$, 3.4 Hz, H-9b), 6.10 (dd, 1H, $J = 9.0$, 2.2 Hz, H-5), 6.21 (d, 1H, $J = 2.2$, H-3), 6.83 (d, 1H, $J = 9.0$, H-6), 7.04–7.48 (m, 10H, H-11, 12, 13, B-Ar), 7.46 (s, 1H, H-7). ^{13}C NMR (75.46 MHz, CDCl$_3$) [δ, ppm]: 13.02 (CH$_3$), 44.93 (CH$_2$), 66.05 (C-8), 71.16 (C-9), 99.16 (C-5), 104.79 (C-6), 108.28 (C-1), 126.89 (C-11), 127.45 (C-12), 129.41 (C-13), 131.58 (C-m), 133.38 (C-p), 134.46 (C-o), 135.46 (C-2), 138.01 (C-10), 153.79 (C-4), 162.26 (C-7), 164.80 (C-2). ^{11}B NMR (86.68 MHz, CDCl$_3$) [δ, ppm]: 2.1. MS (*m/z*, %): 398 (M$^+$, 10), 367 (5), 321 (100), 277 (14.7), 222 (4.5), 91 (5). Anal. calc. for: C$_{25}$H$_{28}$N$_2$O$_2$B: C, 75.20; H, 7.07; N, 7.02. Found: C, 75.10; H, 6.89; N, 6.85%.

2.1.4. (2S,5R)-2-(Phenyl)benzo[j]-5-phenyl-6-aza-1,3-dioxa-2-boracyclononene-6-ene (4b)

Compound **4b** was synthesized from 0.30 g (1.55 mmol) of **3b** and 0.18 g (1.55 mmol) of phenyl boronic acid. The reaction was carried out by refluxing 18 h in toluene. The product was obtained as a yellow solid 0.29 g (1.04 mmol) in 67% yield, m.p. 194–202 °C. IR v_{max} (KBr): 3061, 2930, 2868, 1641 (C=N), 1553, 1472, 1451, 1315, 1263, 1170, 1070, 1022, 859, 753, 702, 650, 526, 474 cm^{-1}. ^{1}H NMR (300 MHz, DMSO-d$_6$) [δ, ppm]: 2.36 (CH$_3$), 4.02 (dd, 1H, $J = 7.7$ Hz, 3 Hz, H-9a), 4.58 (dd, 1H, $J = 7.7$ Hz, 3 Hz, H-9b), 5.05 (dd, 1H, $J = 7.7$ Hz, 3 Hz, H-8), 6.88 (t, 1H, $J = 8.0$ Hz, H-5), 7.01 (d, 1H, $J = 8.0$ Hz, H-3), 7.06–7.09 (m, 2H, H-12, H-14), 7.18–7.20 (m, 3H, H-18, H-19, H-20), 7.24–7.27 (m, 3H, H-6, H-11, H-15), 7.39–7.42 (m, 3H, H-4, H-17, H-21), 7.48 (dd, 1H, $J = 8.0$ Hz, 3 Hz, H-6). ^{13}C NMR (75.46 MHz, DMSO-d$_6$) [δ, ppm]:18.56 (CH$_3$), 65.71 (C-8), 70.49 (C-9), 119.22 (C-5), 120.76 (C-1), 121.13 (C-3), 127.32 (C-12, 14), 127.35 (C-19), 127.64 (C-18, 20), 128.21 (C-6), 128.26 (C-13), 129.27 (C-11, 15), 131.55 (C-17, 21), 136.86 (C-4), 138.30 (C-10), 159.70 (C-2), 169.90 (C-7). ^{11}B NMR (86.68 MHz, CDCl$_3$) [δ, ppm]: 6.1 (h$_{1/2}$ = 396 Hz.). MS (*m/z*, %): 341 (M$^+$, 0.3), 310 (4), 264 (100), 236 (2), 162 (20). Anal. calc. for C$_{22}$H$_{20}$BNO$_2$: C, 77.44; H, 5.91; N, 4.11. Found: C, 77.93; H, 5.87; N, 4.11%.

2.1.5. (2R,5R,11R,14R)-2,11-Oxo-4,4'-bisdiethylaminobenzo[j]-5,14-diphenyl-6,15-diaza-1,3,10,12-tetraoxa-2,11-diboracyclooctadeca-7,16-diene (5)

Compound **5** was synthesized from 0.50 g (1.60 mmol) of **3a** and 0.10 g (1.60 mmol) of boric acid. The reaction was carried by refluxing 18 h in toluene, using a Dean-Stark trap. The product was obtained as a yellow solid (0.41 g, 0.62 mmol) in 78% yield, m.p. 225–226 °C. IR v_{max} (KBr): 3209, 2854, 1640 (C=N), 1354, 1256, 1178, 1160, 1135, 1025, 768, 568 cm^{-1}. ^{1}H NMR (300 MHz, CDCl$_3$) [δ, ppm]: 1.11 (t, 6H, $J = 8.1$ Hz, CH$_3$), 3.31 (q, 4H, $J = 8.1$ Hz, CH$_2$), 3.84 (dd, 1H, $J = 10.0$, 9.3 Hz, H-8), 4.67 (dd, $J = 10.0$, 2.2 Hz, 1H, H-9a), 5.33 (dd, 1H, $J = 9.3$, 2.2 Hz, H-9b), 6.03 (dd, 1H, $J = 8.1$, 2.2 Hz, H-5), 6.10 (d, 1H, d, $J = 2.2$, H-3), 6.71 (d, 1H, $J = 8.1$, H-5) 7.26–7.41 (m, 5H, H-11, 12, 13), 7.35 (s, 1H, H-7). ^{13}C NMR (75.46 MHz, CDCl$_3$) [δ, ppm]: 12.73 (CH$_3$), 44.73 (CH$_2$), 66.58 (C-8), 98.45 (C-5), 103.86 (C-6), 106.24 (C-1), 128.52 (C-11), 128.71 (C-12), 129.53 (C-13), 133.11 (C-2), 136.99 (C-10), 154.74 (C-4), 158.38 (C-2), 161.99 (C-7). ^{11}B NMR (86.68 MHz, CDCl$_3$) [δ, ppm]: 4.0. MS (*m/z*, %): 658 (5), 509 (4.4), 453 (5), 379 (3), 321 (100), 308 (57), 277 (13.1), 204 (12.6), 91 (98). Anal. calc. for: C$_{38}$H$_{46}$N$_4$O$_5$B: C, 69.11; H, 7.02; N, 8.48. Found: C, 69.00; H, 7.05; N, 8.22%.

2.2. Theoretical methods

Gas phase geometries for **5** and **4a** were fully optimized using the GAUSSIAN-98 program package [12] within the framework of the DFT at the B3PW91/6-31G* level [13]. Diethylamino groups were replaced by dimethylamino groups in order to simplify the calculations. The starting parameters for compound **4a** were first taken from the available crystal structure of **4b** (Fig. 3), in which the two phenyl groups are on the same side with respect to the mean plane of the molecule (*cis* isomer). Nevertheless, the *trans* isomer was also envisioned lead-
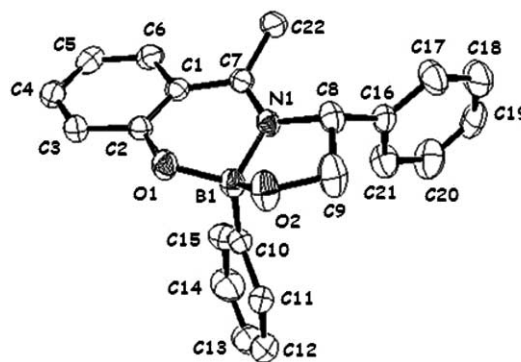
Fig. 3. X-ray molecular structure of compound **4b**, hydrogen atoms are omitted for clarity.

ing to a stabilization of the structure equal to 0.7 kcal. This final configuration was therefore used as the actual structure for the monomeric species.

For the dimeric compound **5**, the starting geometry was built up from that of the oxo-bridged complex **2** [7c], in which two dimethylamino substituents were introduced, together with two phenyl groups in the *pseudo* equatorial position on the lateral alkyl chains. The possibility for having the phenyl in the *pseudo* axial position on the chains was envisioned, but it leads to an overall energy 7.85 kcal higher than that of the *pseudo* equatorial conformation. The model with the phenyl in equatorial position was therefore used as the actual conformation for **5**. Careful examination of the calculated structure revealed that a C_2 symmetry axis is present in the molecule, within an uncertainty of 7×10^{-3} Å. Therefore, the final calculation was performed assuming a C_2 axis, and the resulting structure was chosen as the actual molecular structure for **5**.

Vibrational analyses were performed at the B3PW91/6-31G* level on molecule **4a**, in order to check the presence of a minimum on the potential energy surface, and to compute zero point vibrational energies. These calculations were not carried out on **5**, because of the large size of the molecule. Nevertheless, the two calculated structures are in good agreement with the crystallographic data available (vide infra). Structures **5** and **4a** have been deposited as supplementary materials. The INDO/1 method [14], in connection with the sum-over-states (SOS) formalism [15], was employed for the calculation of the molecular hyperpolarizabilities of both compounds. Details for the efficient INDO-SOS method for the calculation of second order molecular hyperpolazabilities have been reported elsewhere [16].

2.3. NLO measurements

The β measurements were carried out by the electric field induced second harmonic (EFISH) technique [17,18]. The data were recorded using a picosecond Nd:YAG pulsed (10 Hz) laser operating at 1.064 μm. The compounds were dissolved in chloroform at various concentrations (up to 2×10^{-2} mol L^{-1}). The centrosymmetry of the solution was broken by dipolar orientation of the chromophores with a high voltage pulse (5 kV) synchronized with the laser pulse. The SHG signal was selected through a suitable interference filter, detected by a photomultiplier, and recorded on an ultrafast Tektronic TDS 620 B oscilloscope. The NLO response being induced by dipolar orientation, the EFISH signal is related to μ, dipole moment of the chromophores. Therefore, μ were measured independently by a classical method based on the Guggenheim theory [19]. Additionally, the solid state SHG efficiency was evaluated by the Kurtz–Perry powder test [20]. The sam-

ples were uncalibrated powders placed between two glass plates.

3. Results and discussion

3.1. Synthesis

The preparation of monomeric boronates (**4a** and **4b**) and dimeric oxo-bridged compound **5** was carried out as described in the literature for similar compounds [21], by initial formation of the Schiff base and subsequent condensation with the corresponding arylboronic acid or boric acid (Scheme 1) and the compounds were fully characterized by spectroscopic techniques. The existence of the N → B coordination bond was established by ^{11}B NMR, which shows the characteristic signal at 4.0, 2.1 and 6.1 ppm for **5**, **4a** and **4b,** respectively. The signals at 7.35 and 7.46 ppm for **5** and **4a** in the ^{1}H NMR spectrum and 173.97, 162.26, 169.90, 161.99 ppm for **3b**, **4a**, **4b** and **5** in ^{13}C NMR confirmed the imine moiety. The dimeric and monomeric structures were based on mass spectrometry data.

3.2. X-ray structure of compound 4a

The X-ray structure of compound **4b** is shown in Fig. 3, selected bond lengths and angles are summarized in Table 2. The N → B distance for **4b** is 1.590 (2) Å, similar to that observed in other boron complexes [7]. The structure of **4b** shows that both phenyl groups are located on the same side of the molecule (*cis* isomer). The configuration on the newly formed chiral boron atom is *S* and was established with respect to the configuration of the known stereogenic center in (*R*)-phenylglycinol. The O2 presents a weak intermolecular interaction with a methyl hydrogen (H22A), with a distance of 2.447(3) Å which is less than the sum of the van der Walls radii [22]. The angle between O2–H22A–C22 is 137.4° (Fig. 4).

Table 2
Selected bond distances (Å) and angles (°) for compound **4b**

Bond distances			
O(1)–B(1)	1.475(2)	O(1)–C(2)	1.343(2)
O(2)–B(1)	1.442(2)	O(2)–C(9)	1.420(2)
N(1)–B(1)	1.590(2)	N(1)C(7)	1.288(2)
N(1)–C(8)	1.482(2)	B(1)–C(15)	1.608(3)
Bond angles			
C(2)–O(1)–B(1)	118.03(12)	C(9)–O(2)–B(1)	107.27(14)
C(7)–N(1)–B(1)	124.07(14)	C(8)–N(1)–B(1)	108.41(14)
C(7)–N(1)–C(8)	125.63(15)	O(2)–B(1)–O(1)	110.34(14)
O(1)–B(1)–N(1)	107.07(15)	O(2)–B(1)–N(1)	99.83(14)
O(1)–B(1)–C(15)	111.93(14)	O(2)–B(1)–C(15)	114.65(17)
N(1)–B(1)–C(15)	112.19(13)	O(1)–C(2)–C(1)	122.20(14)
C(2)–C(1)–C(7)	118.11(15)	N(1)–C(7)–C(1)	116.91(15)
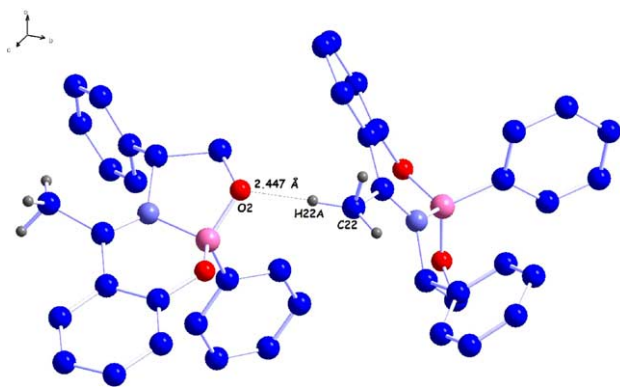
Fig. 4. Intermolecular interactions in the X-ray crystal structure of compound **4b**.

3.3. Calculated structures

The most striking difference between the calculated (**4a**) and experimentally determined (**4b**) monomeric structures is the relative configuration of the two phenyl substituents, which are on the same side of the molecular mean plane in the X-ray structure, while calculations show that they are more stable on opposite sides. Nevertheless, the *cis* and *trans* isomers of **4a** exhibit nearly identical UV–visible spectra, strongly dominated by the aminosalicylaldiminato fragment, which is responsible for the charge transfer process. Therefore, the effect of these structural features on the NLO response of **4a** is probably negligible.

The structure of the oxo-bridged compound **5** is closely related to that of the model structure **2**. In particular, the angle between the two salicylaldiminato fragments in **2** (82°, X-ray data) is not significantly modified after introduction of the phenyl substituents in the calculated structure of **5**. The hypothetical isomer in which the phenyl groups occupy axial positions with respect to the *YZ* plane (Fig. 2) also exhibit a strongly bent structure. On the other hand, its energy is 7.85 kcal higher than that of the isomer having the phenyl in equatorial position, therefore, it was not considered in the present investigation.

In order to compare the mono- (**4a**) and di-boronated derivatives (**5**), the coordination spheres around the boron atoms are presented in Table 3 along with the

X-ray data available. The agreement between the calculated and experimental values is satisfactory. The calculated bond lengths are approximately the same for the boron-salicylaldiminato units of both the mono- and di-boronated species, the main difference corresponds to the B–N distance which has a calculated value of 1.611 and 1.597 Å in **5** and **4a**, respectively. This difference in bond lengths has the potential to modify the NLO response as the coordination to nitrogen is usually associated to an increase in electron withdrawing effect [23]. Thus the decrease in boron nitrogen distance calculated in **4a** should lead to an enhancement of the intramolecular ($Me_2N- \rightarrow -C=N$) charge transfer to a larger wavelength, and hence to a larger β value. However, the bond shortening is very weak (0.014 Å) and its overall contribution is probably modest. Therefore, the observation of roughly similar structural features leads to the conclusion that the charge transfer processes should have the same origin in **5** and **4a**.

3.4. Spectroscopic properties

The experimental absorption spectra for **5** and **4a** recorded in chloroform are presented in Fig. 5, while experimental and ZINDO spectra are compared in Table 4. The mono-boronated derivative **4a** exhibits an intense band (*A*) at 391 nm ($\varepsilon = 54\,000$ L mol^{-1} cm^{-1}). An additional and less intense transition (*B*) is observed at 348 nm ($\varepsilon = 25\,000$ L mol^{-1} cm^{-1}). Although there is a shift of about 30 nm between the experimental and calculated spectra, it falls within the standard range of uncertainty (about 50–100 nm) observed in ZINDO calculation of Schiff base complexes [24]. Therefore, the agreement is found to be satisfactory. On passing from the mono- to the di-boronated compound, both experimental and calculated spectra reveal a slight blue shift and a large enhancement of the intensity. The experimental wavelength difference between *A* and *B* is strongly reduced from 43 to 16 nm in **5**. This behavior is observed on the calculated spectra as well, but to a far less extent (53–43 nm). Finally, a new band (*C*) is observed in **5**, which is absent in the related compound **4a**.

The origin of the electronic transitions in **4a** can be understood from the analysis of the ZINDO spectrum (Table 4), which relates band *A* to a single low lying

Table 3

Relevant calculated (DFT) and experimental (X-ray) bond lengths (Å) and angles (°) in the coordinated sphere of the boron atom for the mono- (**4a**, **4b**) and di-boron derivatives (**5**, **2**)

	4a(DFT)	**4b**(X-ray)	**5**(DFT)		**2**(X-ray)	
B–O(phenol)	1.499	1.492(2)	B–O(phenol)	1.498	1.487(3)	1.493(3)
B–O(alcohol)	1.451	1.475(2)	B–O(alcohol)	1.445	1.437(3)	1.438(3)
B–N	1.597	1.590(2)	B–N	1.611	1.611(3)	1.603(3)
B–C	1.616	1.608(3)	B–O(oxo)	1.412	1.416(3)	1.414(3)
O(phenol)–B–N	105.5	107.1(1)	O(phenol)–B–N	108.2	107.9(2)	107.6(2)
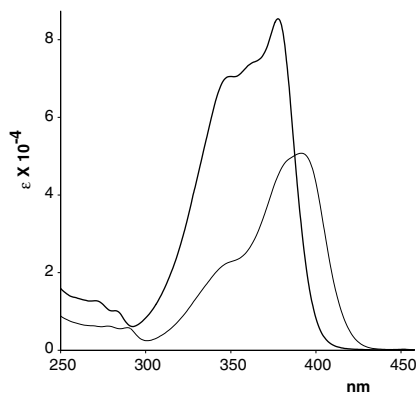
Fig. 5. Absorbance spectra for **5** (bold line) and **4a**, measured in CHCl₃.

$1 \rightarrow 2$ transition having a strong HOMO (aminophenyl) $\rightarrow$ LUMO (imine) character. Similarly, band B is ascribed to the $1 \rightarrow 3$ transition having a strong HOMO-3 (aminophenyl) $\rightarrow$ LUMO (imine) character. Both transitions will therefore result in a net charge transfer process responsible for the NLO response of compound **4a**.

The oxo-bridged derivative **5** reveals a spectrum of a much greater complexity than that of the parent compound **4a**. However, a careful analysis indicates that, to a large extent, the electronic properties of **4a** can easily be transposed to **5** (by linear combination within a C_2 symmetry). Thus each orbital in **4a** can find its counterpart in **5**, as a set of two nearly degenerated orbitals, symmetric and antisymmetric combinations of the contribution of mono-boronated subunits. For example, orbital 113 (in **5**) is the symmetric combination of two identical orbital fragments having an electron distribution reminiscent of that of orbital 70 (in **4a**), while orbital 114 is the antisymmetric combination of the same orbital fragments. Consequently, the charge transfers associated to bands A and B in **5** have the same atomic origin as those observed in **4a**. Nevertheless, and for symmetry reasons, the overall charge transfer process (and hence the NLO properties) necessarily arises from the projection of the subunit contributions along the twofold axis.

In the above description, the role devoted to band C has been neglected in compound **5**. Nevertheless, the ZINDO analysis indicates the presence of a transition ($1 \rightarrow 8$, Table 4) with reduced intensity (f) and higher energy (E) than those associated to bands A and B. This should result in a modest contribution to the NLO response, assumed to be proportional to the f/E^3 [3] factor [5,17a]. It is therefore reasonable to infer from this comparison that the origin of the NLO behavior is roughly the same in **5** and **4a**.

3.5. NLO properties of **4a** and **5**

Within the assumption of charge transfer processes closely related in **4a**, and in the salicylaldimine subunits of **5**, the change in the molecular hyperpolarizabilities on passing from the mono- to the di-boronated species can be evaluated from the examination of the molecular structures. In chromophores exhibiting "push-pull" character (**4a**), the β tensor can be restricted to a single tensor component along a charge transfer axis. Therefore, $\beta_{(4)}$ is a vector roughly oriented along the $Et_2N– \rightarrow –C{=}N$ direction. In the case of **5**, the actual C_2 symmetry imposes that β is strictly parallel to the symmetry axis. Therefore $\beta_{(3)} = 2 \times \beta_{(4)} \times \cos\theta$ (θ being the angle between the charge transfer axis of one molecular subunit ($Et_2N– \rightarrow –C{=}N$ direction) and the twofold axis of compound **5**). Although it is not obvious to calculate θ very precisely, one may necessarily state that $\theta \geqslant 41°$ (the angle value calculated between the salicylaldimine planes and the twofold axis). This leads to $\beta_{(3)} \leqslant 1.5\beta_{(4)}$.

The experimental (EFISH) β measurements for **4a** and **5** are gathered in Table 5. The data indicate that β is roughly doubled on passing from the mono- (**4a**) to the di-boronated (**5**) derivative, in striking contrast with the above prediction. However, one has to be reminded that in many NLO processes (e.g., in the widely investigated poled polymer materials [25], or in the present EFISH measurements), the relevant molecular parameter is not β, but β_{vec}, projection of β along the molecular dipole moment (μ). In other words, β_{vec} becomes the only part of the molecular nonlinearity, which contributes to the effective NLO property in that

Table 4
Analysis of the ZINDO computed data for the low-lying transitions of **5** and **4a**

	Band	Transitions	λ_{max}	Oscillator strength	Experimental	Main components in the CI expansion[a]
5	A	$1 \rightarrow 2$	343	0.43	377 (89 000)	$0.644\chi_{114 \rightarrow 115} + 0.595\chi_{113 \rightarrow 116}$
		$1 \rightarrow 3$	341	0.40		$-0.604\chi_{114 \rightarrow 116} - 0.564\chi_{113 \rightarrow 115}$
	B	$1 \rightarrow 4$	300	0.31	361 (83 000)	$-0.551\chi_{112 \rightarrow 115} + 0.506\chi_{111 \rightarrow 116}$
		$1 \rightarrow 5$	297	0.41		$-0.501\chi_{112 \rightarrow 116} + 0.466\chi_{111 \rightarrow 115}$
	C	$1 \rightarrow 8$	253	0.25	347 (74 000)	$0.516\chi_{114 \rightarrow 121} - 0.506\chi_{113 \rightarrow 122}$
4a	A	$1 \rightarrow 2$	363	0.39	391 (54 009)	$0.867\chi_{70 \rightarrow 71}$
	B	$1 \rightarrow 3$	310	0.35	348 (25 000)	$0.697\chi_{67 \rightarrow 71}$

Experimental (λ_{max} in nm, and ε in L mol⁻¹ cm⁻¹), ZINDO calculated (λ_{max} and oscillator strength f).
[a] 114 is the HOMO and 115 the LUMO in **3**. 70 is the HOMO and 71 the LUMO in **4**.

Table 5
EFISH data (β in cm^5 esu^{-1} and μ in D) for **5** and **4a**, recorded at 1.064 μm

	β	μ
5	19.5×10^{-30}	4.0
4a	9.8×10^{-30}	5.1

case, due to the polar BO_2 inorganic core, there is no reason that β and μ are strictly parallel in **4a**, therefore, the effective hyperpolarizability (β_{vec}) may be significantly reduced, versus the total molecular NLO response (β). By contrast, this effect is inoperative in **5**, where the presence of a twofold axis imposes that the major component of β is along the dipole moment. As a consequence, β_{vec} is strictly equal to β, making a better use of the entire optical nonlinearity potentially available. Along this line, the actual symmetry axis reinforces the NLO properties of $\beta_{(3)}$ as determined by EFISH which becomes twice as large as $\beta_{(4)}$.

Finally, to test the suitability of our two step strategy aimed at (i) combining two $Et_2N-\rightarrow-C\equiv N$ charge transfers in a non-centrosymmetric molecular geometry, and (ii) engineering the molecules in a non-centrosymmetric solid state environement by means of chirality, the SHG efficiency of **5** in the solid state has been measured. Unfortunately, the crystallinity is quite poor, which leads to a modest efficiency around 0.8 times that of urea. All our attempts towards microcrystalline powder of better quality were unsuccessful. This illustrates the limitation of the strategy based on non-centrosymmetric crystallization in nonlinear optics.

4. Conclusion

Two new chiral boronates were prepared easily and in good yields. This approach gives a convenient way to prepare chiral moieties for NLO purposes. The experimental quadratic hyperpolarizability is roughly twice as large in **5** than in its parent mono-boronated **4a**, which indicates that oxo-bridged di-boronated cores could be successfully used to engineer various "push-pull" salicylaldiminato based ligands in a non-centrosymmetric molecular environment. A slight blue-shift observed in the di-boronated species is evidenced as a side effect for this unusual complexation mode. It could lead to an enlargement of the transparency domain, which becomes an interesting electronic feature when NLO properties are being considered.

Acknowledgments

Appendix A. Supplementary data

Calculated structures for **4a** and **5**. Crystallographic data for **4b** have been deposited at the Cambridge Crystallographic Data Centre with deposition number 259940. Copies of the information may be obtained free of charge from The Director, CCDC, 12 Union Road, Cambridge CB2 1EZ, UK (fax: +44 1223 336 033; e-mail: deposit@ccdc.cam.ac.uk or http://www.ccdc.cam.ac.uk). Supplementary data associated with this article can be found, in the online version, at doi:10.1016/j.jorganchem.2005.05.034.

References

[1] M.F. Hawthorne, M.W. Lee, J. Neurooncol. 62 (2003) 33.
[2] (a) M. Suginome, L. Uehlin, A. Yamamoto, M. Murakami, Org. Lett. 6 (2004) 1167;
(b) J.W.J. Kennedy, D.G. Hall, Angew. Chem. Int. Ed. 42 (2003) 4732.
[3] Z. Liu, Q. Fang, D. Cao, D. Wang, G. Xu, Org. Lett. 6 (2004) 2933.
[4] (a) C.D. Entwistle, T.B. Marder, Angew. Chem. Int. Ed. 41 (2002) 2927;
(b) H. Reyes, B.M. Muñoz, N. Farfán, R. Santillan, S. Rojas-Lima, P.G. Lacroix, K.J. Nakatani, J. Mater. Chem. 12 (2002) 2898.
[5] J.L. Oudar, D.S. Chemla, J. Chem. Phys. 66 (1977) 2664.
[6] D.J. Williams, Angew. Chem., Int. Ed. Engl. 23 (1984) 690.
[7] (a) H. Höpfl, N. Farfán, J. Organomet. Chem. 547 (1997) 71;
(b) N. Farfán, H. Höpfl, V. Barba, M.E. Ochoa, R. Santillan, E. Gómez, A. Gutiérrez, J. Organomet. Chem. 581 (1999) 70;
(c) V. Barba, G. Vargas, E. Gómez, N. Farfán, Inorg. Chim. Acta 311 (2000) 133.
[8] G.M. Sheldrick, University of Göttingen: Göttingen, 1993.
[9] A.L. Spek, J. Appl. Cryst. 36 (2003) 7.
[10] L. Farrugia, J. Appl. Cryst. 32 (1999) 837.
[11] L. Farrugia, J. Appl. Cryst. 30 (1997) 565.
[12] M.J. Frisch, G.W. Trucks, H.B. Schlegel, G.E. Scuseria, M.A. Robb, J.R. Cheeseman, V.G. Zakrzewski, J.A. Montgomery Jr., R.E. Stratmann, J.C. Burant, S. Dapprich, J.M. Millam, A.D. Daniels, K.N. Kudin, M.C. Strain, O. Farkas, J. Tomasi, V. Barone, M. Cossi, R. Cammi, B. Mennucci, C. Pomelli, C. Adamo, S. Clifford, J. Ochterski, G.A. Petersson, P.Y. Ayala, Q. Cui, K. Morokuma, D.K. Malick, A.D. Rabuck, K. Raghavachari, J.B. Foresman, J. Cioslowski, J.V. Ortiz, A.G. Baboul, B.B. Stefanov, G. Liu, A. Liashenko, P. Piskorz, I. Komaromi, R. Gomperts, R.L. Martin, D.J. Fox, T. Keith, M.A. Al-Laham, C.Y. Peng, A. Nanayakkara, C. Gonzalez, M. Challacombe, P.M.W. Gill, B. Johnson, W. Chen, M.W. Wong, J.L. Andres, C. González, M. Head-Gordon, E.S. Replogle, J.A. Pople, GAUSSIAN 98, Revision A.9, Gaussian Inc., Pittsburgh, PA, 1998.
[13] (a) A.D. Becke, J. Chem. Phys. 98 (1993) 1372;
(b) J.P. Perdew, Y. Wang, Phys. Rev. B 45 (1992) 13244.
[14] (a) M.C. Zerner, R.F. Loew, G. Kirchner, U. Mueller-Westerhoff, J. Am. Chem. Soc. 102 (1980) 589;
(b) P. Anderson, D. Edwars, M.C. Zerner, Inorg. Chem. 25 (1986) 2728.

[15] J.F. Ward, Rev. Mod. Phys. 37 (1965) 1.

[16] D.R. Kanis, M.A. Ratner, T.J. Marks, Chem. Rev. 94 (1994) 195.

[17] (a) J.L. Oudar, J. Chem. Phys. 67 (1977) 446;
(b) B.F. Levine, C.G. Betha, J. Chem. Phys. 63 (1975) 2666;
(c) B.F. Levine, C.G. Betha, J. Chem. Phys. 65 (1976) 1989.

[18] I. Maltey, J.A. Delaire, K. Nakatani, P. Wang, X. Shi, S. Wu, Adv. Mater. Opt. Electron. 6 (1996) 233.

[19] E.A. Guggenheim, Trans. Faraday Soc. 45 (1949) 714.

[20] (a) S.K. Kurtz, T.T. Perry, J. Appl. Phys. 39 (1968) 3798;
(b) J.P. Dougherty, S.K. Kurtz, J. Appl. Crystallogr. 9 (1976) 145.

[21] V. Barba, G. Vargas, E. Gómez, N. Farfán, Inorg. Chim. Acta 311 (2000) 133.

[22] A. Bondi, J. Phys. Chem. 68 (1964) 441.

[23] (a) See for example: M.J. Gerard, A. Woodward, N.J. Taylor, T.B. Marder, I. Cazenobe, I. Ledoux, J. Zyss, A. Thornton, D.W. Bruce, A.K. Kakkar, Chem. Mater. 10 (1998) 1355;
(b) D.R. Kanis, P.G. Lacroix, M.A. Ratner, T.J. Marks, J. Am. Chem. Soc. 116 (1994) 10089.

[24] (a) J.P. Costes, J.F. Lamère, C. Lepetit, P.G. Lacroix, F. Dahan, Inorg. Chem. 44 (2005) 1973;
(b) P.G. Lacroix, I. Padilla-Martínez, H. López Sandoval, K. Nakatani, New J. Chem. 28 (2004) 5421.

[25] (a) R. Dagani, Chem. Eng. News, March 4, 1996, p. 22.;
(b) M. Eich, G.C. Bjorklund, D.Y. Yoon, Polym. Adv. Technol. 1 (1990) 189.